

See discussions, stats, and author profiles for this publication at: <https://www.researchgate.net/publication/236619131>

# Fractal Nature of Simulated Lightning Channels

Article in Sri Lankan Journal of Physics · December 2012

DOI: 10.4038/sljip.v13i2.5433

---

CITATIONS

9

---

READS

206

2 authors, including:



**Upul Sonnadara**

University of Colombo

203 PUBLICATIONS 1,917 CITATIONS

SEE PROFILE

Some of the authors of this publication are also working on these related projects:



World bank Sector work in Sri lanka [View project](#)



INSTITUTE OF PHYSICS - SRI LANKA

## **Research Article**

# **Fractal Nature of Simulated Lightning Channels**

**M.D.N. Perera and D.U.J. Sonnadara\***

*Department of Physics, University of Colombo, Colombo 00300, Sri Lanka.*

---

### **Abstract**

Cloud-to-ground lightning discharges in 2D and 3D domains were simulated using a stochastic dielectric breakdown model. The dependency between fractal dimension of the discharge patterns and the power of the local electric field  $\eta$  was critically evaluated. An exponential decrease in fractal dimension was observed as  $\eta$  increases. Fractal dimension of simulated 3D discharge patterns and 2D images of lightning discharges were compared by taking projections of simulated patterns. Discharge patterns similar to actual lightning were obtained when  $\eta \approx 5.2$ . Influence of ground objects on simulated lightning discharges was also studied by introducing additional boundary conditions to the ground plane. It was observed that pointed structures on the ground have a higher probability of attracting simulated lightning discharges. An extension was introduced to dielectric breakdown model to simulate the development of upward connecting positive leader discharges that occur during the decent of a downward moving negative leader. It was found that the height of the stepped leader tip above the ground (at the time when the upward connecting leader initiation occurs) is dependent on the initial breakdown voltage threshold. The height of the point of interception was found to decrease exponentially as the breakdown threshold is increased.

**Keywords:** Dielectric breakdown, Fractal dimension, Electrical discharges

---

## **1. INTRODUCTION**

Electrical discharges that occur during the breakdown of all gaseous, liquid and solid dielectrics are recognized as having a strong tendency to develop into complex branched structures. Various categories of discharges such as lightning, surface discharges, and treeing in polymers occur as trajectories of luminous filaments, which often branch into intricate patterns. Although there are fundamental differences between discharge mechanisms of those various discharge types, global structure of the branched tree-like patterns often shows a close structural similarity within a large variety of discharge types<sup>1</sup>.

---

\* Corresponding Author E mail: upul@phys.cmb.ac.lk

Due to the large number of highly non-linear phenomena that occurs from atomic scale to macroscopic scale during the breakdown process, providing an adequate description about the formation of these complex geometrical structures with the classical theory of discharges has been a much difficult task, and it still remains unaccomplished, as up to today<sup>2</sup>.

However, the theory of fractal geometry introduced in the late 1970's by Benito Mandelbrot<sup>3</sup> provided a means of characterizing variety of complex patterns that encounter in nature. Mandelbrot brought up the geometrical difference between Euclidean shapes and so called *fractals*, and categorized complex, self-similar natural structures such as clouds, trees, mountain ranges, river networks as fractal shapes having non-integer *fractal dimension*. The concept *fractal dimension* could be used to quantitatively characterize and classify random complex patterns, and served as a means of categorizing an object as a fractal.

Since the theory of fractals has been popularized, many attempts have been made to relate the branching self-similar patterns observed in electrical discharges with fractals. Niemeyer *et al.*<sup>1</sup> presented evidence for fractal properties of branched discharges by analyzing simulated surface discharge patterns. Their analysis suggested that surface discharges are indeed fractal structures with average fractal dimension  $D \approx 1.7$ . By analyzing a set of lightning photographs, Tsonis<sup>4</sup> reported that the average fractal dimension of projected images of lightning flashes is  $D \approx 1.34$ .

With the confirmation of the fractal nature of electrical discharges, stochastic models were introduced to describe the formation of branched discharge patterns. By combining the potential theory with probabilistic selection, these models were able of produce complex branched structures that resemble actual electrical discharges. The work presented in this paper utilizes a stochastic model to simulate the formation of lightning discharges in both two dimensional (2D) and three dimensional (3D) domains. The standard model<sup>5-7</sup> was extended to simulate the interception of downward moving negative leader channel and upward connecting positive leader discharges. Using the simulated data, the fractal dimension of the simulated lightning channels is investigated.

## 2. METHODOLOGY

### 2.1 Previous work

Niemeyer *et al.*<sup>1</sup> introduced *Dielectric Breakdown Model* (DB model) to explain fractal properties observed in surface discharges in compressed SF<sub>6</sub> gas. The basic assumption of their stochastic model was that the discharge pattern exhibits fractal scaling if two mathematical conditions are satisfied.

- Probability of growth at any point of the discharge is proportional to a power of the local electric field at that point.
- The discharge structure is equipotential. i.e., the voltage gradient along the structure is zero.

Niemeyer *et al.* studied their model via computer simulations in a 2D square lattice under 2D Laplacian field, and obtained highly branched structures similar to experimental surface discharge patterns when the power ( $\eta$ ) is set to 1. They estimated the fractal dimension of their simulated discharge patterns to be  $1.75 \pm 0.02$  which was in good agreement with the value 1.7, suggested by fractal analysis of experimental surface discharge patterns. They further studied the effect of the values of  $\eta$  other than 1 and observed that the density of the branching in the discharge pattern decreases as  $\eta$  increases. i.e., the fractal dimension decreases as  $\eta$  increases.

Sanudo *et al.*<sup>5</sup> extended the two dimensional DB model to simulate lightning discharges in three dimensions and estimated the average fractal dimension in 3D as well as the average fractal dimension of 2D vertical projections of discharge patterns. They studied the relationship between  $\eta$  and the fractal dimension and reported that 2D projection of simulated lightning discharges with  $\eta \approx 6$  has the average fractal dimension of 1.34; the value observed in actual lightning photographs.

Mansell *et al.*<sup>8</sup> also extended the DB model to a 3D Cartesian geometry to simulate lightning discharges. In addition, they integrated the DB model with a numerical cloud model to study lightning behaviour during thunderstorms.

Kim *et al.*<sup>9</sup> proposed a novel extension to the DB model in order to animate sustained electrical arcs, by assuming the existence of residual positive charge along discharge channels. With their improvements, they were able to simulate subsequent dart leaders that follow the same general path as the stepped leader in lightning flashes.

In a more recent work by Kim *et al.*<sup>10</sup> a faster; more memory efficient algorithm was introduced to simulate electrical discharges. Their algorithm was structurally similar to DB model, with the exception that the discharge structure is treated as a perfect insulator, instead of a conductor. With this modification, they were able to replace the most time consuming numerical step of DB model; solving Laplace equation under finite difference method; with a fast analytical method. They compared the performance of their algorithm with original DB model algorithm and reported that in general their algorithm is 651 times faster than the original DB model.

## 2.2 Dielectric breakdown model

Lightning discharge simulations presented in this paper are based on a generalized version of the original Dielectric Breakdown Model developed by Niemeyer *et al.* [1]. DB model is defined in discrete coordinate space. Figure 1 shows a sample square lattice (in its initial state) used to produce lightning discharge patterns in 2D. Discharge pattern is indicated by black circles connected with thick lines. Dashed lines which connect each discharge point (black circle) with a neighboring charge-free lattice point (white circle) represent possible breakdown links.

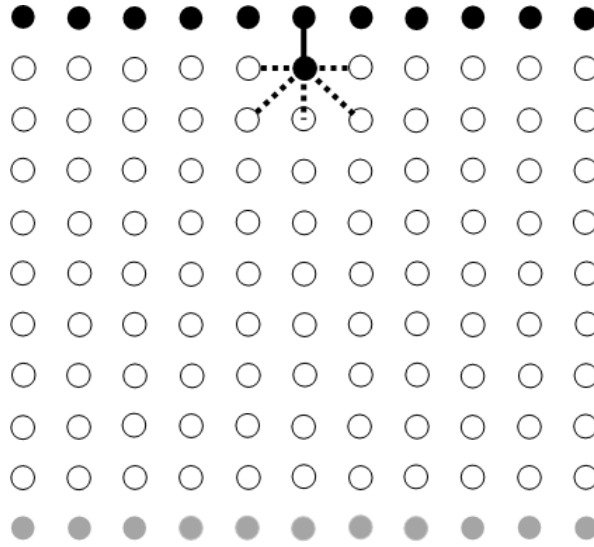


**Figure 1:** Initial charge configuration for producing downward moving negative leaders.

Each lattice point has an electric potential value  $\phi$  associated with it. The potential of the lattice points in the upper boundary of the lattice (which simulates the cloud base) are fixed to  $\phi = U_{\text{cathode}}$ , while lattice points in the lower boundary (which simulates the ground plane) are fixed to  $\phi = U_{\text{anode}}$ . As for the left and right boundaries, Neumann boundary conditions ( $\partial\phi/\partial x = 0$ ) are imposed. Potential of the remaining charge-free lattice points (white circles) are defined by the discrete Laplace equation under the boundary conditions imposed by the cloud base, ground plane and the discharge structure developed up to that time.

DB model is an iterative process. The process starts with the initial boundary conditions consist of the negative cloud base and the positive ground plane. The central lattice point of the upper boundary is capable of initiating the discharge. During each iteration of the algorithm, a new breakdown link (dashed line segment) is chosen and added to the existing discharge pattern. The new breakdown links are chosen randomly according to a weighted probability function as described below.

Let  $P$  denote a lattice point connected to the discharge pattern (black circle) while  $Q$  represents an adjacent charge-free lattice point (white circle). Magnitude of the

component of electric field vector (local electric field) at  $P$  pointing in the direction of  $PQ$  is approximated by;

$$E_{PQ} = \frac{|\phi_P - \phi_Q|}{d} \quad (2.1)$$

where  $d$  is the length of a dashed line segment (for simplicity,  $d$  is set to 1).

The probability of choosing a particular  $PQ$  dashed line segment is proportional to a power of the local electric field associated with it.

$$P_{PQ} \propto (E_{PQ})^\eta \quad (2.2)$$

The above probability can be normalized to a value between 0 and 1 by dividing with the sum of probabilities corresponding to all possible breakdown links extend from point  $P$ ;

$$P_{PQ} = \frac{(E_{PQ})^\eta}{\sum_{i=1}^n (E_{(PQ)_i})^\eta} \quad (2.3)$$

When a new breakdown link is selected and a new lattice point is connected to the discharge pattern, the electric potential  $\phi_Q$  of the new discharge point  $Q$  is set to  $U_{\text{cathode}}$ .

Each time a new breakdown link is chosen, the newly added discharge point becomes part of the boundary conditions. Therefore, potential at charge-free lattice points have to be recalculated under the new boundary conditions by solving Laplace equation;

$$\nabla \phi = 0 \quad (2.4)$$

Since Laplace equation is linear, the value of  $\phi$  at any point is the average of those around that point. Thus in a discrete lattice structure, potential at any lattice point is the average potential of its nearest neighbors. Therefore, discrete form of equation 2.4 can be represented as,

$$\phi_{i,j,k} = \frac{1}{6}(\phi_{i+1,j,k} + \phi_{i-1,j,k} + \phi_{i,j+1,k} + \phi_{i,j-1,k} + \phi_{i,j,k+1} + \phi_{i,j,k-1}) \quad (2.5)$$

where  $i, j, k$  represent discrete lattice coordinates.

To increase the speed of convergence, the system of equations generated by equation 2.5 was solved by the technique *successive over-relaxation*<sup>11</sup>. Given the appropriate boundary conditions, potential of the lattice points are computed by iterating equation 2.6 over the lattice (except at boundaries where the potential is fixed) until convergent

results are obtained.

$$\phi_{i,j,k}^{(n)} = \phi_{i,j,k}^{(n-1)} + \frac{\omega}{6} \delta_{i,j,k} \quad (2.6)$$

where;

$$\delta_{i,j,k} = \phi_{i+1,j,k}^{(n-1)} + \phi_{i-1,j,k}^{(n)} + \phi_{i,j+1,k}^{(n-1)} + \phi_{i,j-1,k}^{(n)} + \phi_{i,j,k+1}^{(n-1)} + \phi_{i,j,k-1}^{(n)} - 6\phi_{i,j,k}^{(n-1)} \quad (2.7)$$

Here, the superscript  $(n)$  denotes the current iteration cycle while  $(n-1)$  denote the previous cycle. The over-relaxation parameter  $\omega$  ( $1 \leq \omega \leq 2$ ) controls the speed of convergence. Sanudo *et al.*<sup>5</sup> states that  $\omega \approx 1.6$  considerably increases the speed of convergence of the whole process. Therefore in this study, a value of 1.6 was used for  $\omega$ .

The potential of each lattice point in a 2D lattice can be calculated in sequence by advancing from the left to the right of the lattice in each row and from bottom to top in successive rows. For a 3D lattice the scan in XZ plane should be repeated for each discrete value of Y coordinate by advancing sequentially in the Y direction. A complete scan of the lattice in the above manner constitute one iteration cycle. Iterative scanning process is continued until residual values  $\delta_{i,j,k}$  of all lattice points become less than a threshold value  $m$ . To obtain reasonable convergent results, value of  $m$  was chosen such that the residual values are reduced to a magnitude of 0.1% of the maximum boundary potential.

In order to increase the execution speed, equation 2.6 was first solved for a subsystem of  $20 \times 20 \times 20$  cube, centered at the newly added discharge point. When the 0.1% convergence criterion is reached for this subsystem, the program proceeds to solve the total system consisting of the entire lattice. The above computational trick was based on the observation that the changes in the potential field after the addition of a new discharge point are particularly strong in the surrounding of the new point, while the effect reduces rapidly with distance. In this study, all 3D simulations were executed for a  $100 \times 100 \times 100$  cubic lattice due to execution speed limitations.

### 2.3 Simulating upward connecting leaders

During real lightning flashes, when the stepped leader has approached within 15 to 50 meters of the ground, the electric field intensity at the ground becomes sufficient enough to initiate one or more upward connecting positive leaders which will propagate upwards to meet up with the oncoming negative leader. In this study, DB model was extended to account for the upward connecting positive leaders.

Original DB model introduced by Niemeyer *et al.*<sup>1</sup> only allows unidirectional discharge propagation. However, the generalized DB model presented in this paper implicitly allows the propagation of both negative and positive discharges. The obvious reason for this behavior is that the probability of growth is related to the *magnitude* of the local electric field. Therefore, independent of the type of the discharge, the pattern will tend to develop in the directions with higher potential gradient. That is, negative discharges (which carry negative charge and have lower potential) tend to propagate towards regions of higher potential while positive discharges (which carry positive charge and have higher potential) tend to propagate towards regions of lower potential.

When generating negative discharges, the central point of the upper face of the lattice was chosen as the only discharge initiation point, and the initial set of possible breakdown links were extended from that point. Similarly in order to simulate positive discharges, one or more lattice points comprising the ground plane have to be designated as discharge initiation points, and initial set of possible breakdown links have to be extended from those points. Once the initial set of possible breakdown links are specified, positive discharges will propagate in the same step-by-step manner as the negative discharges.

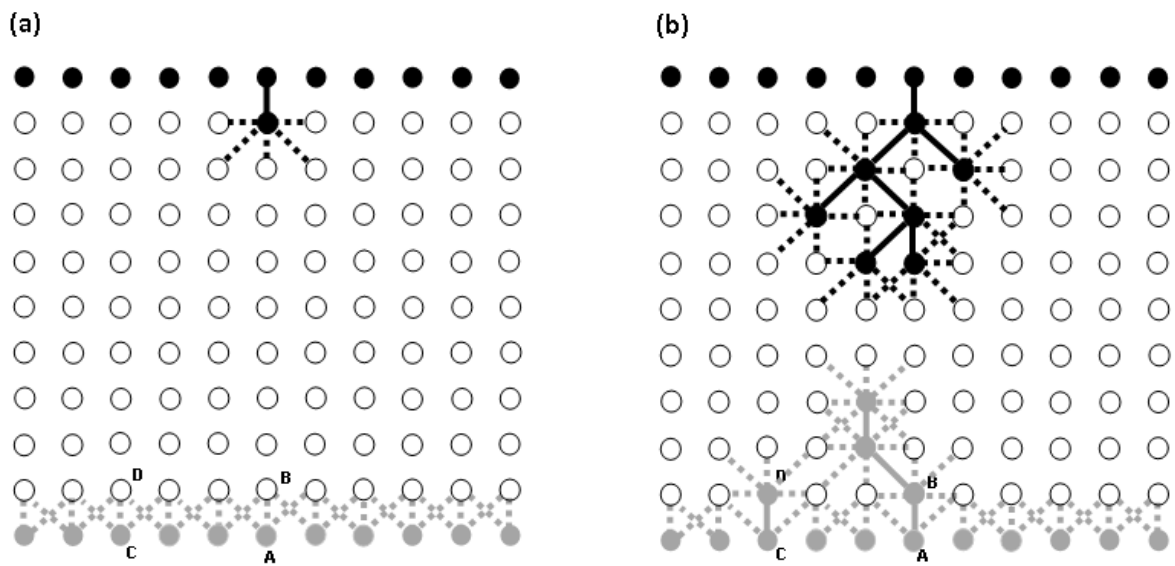
In the original DB model, discharge initiation phase is not explicitly modeled. During the first iteration of the algorithm, it is assumed that the conditions for discharge initiation have already been satisfied by the initial set of possible breakdown links. However in order to simulate the development of upward connecting positive leaders, an explicit initiation condition for positive discharges have to be enforced.

Figure 2a shows the initial state of a 2D sample lattice. All lattice points on the ground layer (anode) are connected to adjacent charge-free lattice points on the layer above to form the initial set of possible breakdown links for positive discharges (indicated by gray colored dashed lines). However, not all those links are capable of being selected as a discharge link. For an initial possible breakdown link to be chosen as a discharge link, local electric field associated with the link must exceed a threshold value  $E_{break}$ . During each iteration, the algorithm scans through the initial set of possible breakdown links to check whether the local electric field associated with any of them have exceeded  $E_{break}$ . If such links exist, one of them will be chosen according to equation 2.3 and added as the first discharge link of a new upward connecting leader (e.g. AB). After the first discharge link of a new upward connecting leader is formed, that leader is allowed to develop according to the same propagation rules as the negative discharge. Note that the threshold  $E_{break}$  only influences the selection of *initial* possible breakdown links. Possible breakdown links formed later in the process are only subjected to the selection rule, equation 2.3.

Propagation of the stepped leader (negative discharge) is the same as in the original DB model. During each iteration of the algorithm, a new negative discharge link is chosen and added to the stepped leader. However during initial iterations, upward connecting



leaders may not be created since the local electric field near the ground plane is not sufficient enough to exceed  $E_{break}$ . But as the stepped leader approaches the ground, electric field near the ground plane will gradually intensify; and at some point, local electric field associated with one or more possible breakdown links will exceed  $E_{break}$ , initiating upward connecting positive leaders. During the time span of the simulation, more than one upward connecting positive leader may develop. Simulation is continued until the downward moving negative leader intercept with one of the upward connecting positive leaders, forming the complete lightning path. Figure 2b shows the lattice configuration after several iterations. At the given time, stepped leader has propagated half way down the lattice, and two upward connecting positive leaders have initiated from AB and CD.



**Figure 2:** A sample 2D lattice showing upward connecting positive leader development (a) Initial charge configuration (b) Configuration after several iterations.

## 2.4 Estimating fractal dimension

In this work, simulated electrical discharges were structurally characterized by calculating the associated fractal dimension. There are number of different methods of calculating fractal dimension of electrical discharges<sup>6</sup>. In this work, method of *correlation function* was employed since it is guaranteed to provide distributions with smaller standard deviations of the fractal dimension<sup>12</sup>.

Method of Correlation function gives a statistical measure for fractal dimension based on pair-wise distance between a set of random points.

Consider a set of  $N$  points in an  $m$ -dimensional space;

$$x_i = [x_i^{(1)}, x_i^{(2)}, \dots, x_i^{(m)}] \quad (2.8)$$

where  $i = 1, 2, 3, \dots, N$

Correlation integral  $C(\varepsilon)$  for the given set of points is defined as;

$$C(\varepsilon) = \lim_{N \rightarrow \infty} \frac{1}{N^2} \sum_{i=1}^N \sum_{j=i+1}^N H(\varepsilon - |x_i - x_j|) \quad (2.9)$$

where  $H$  is the *Heaviside step function*;

$$H(x) = \begin{cases} 0, & x < 0 \\ 1, & x \geq 0 \end{cases} \quad (2.10)$$

In literal terms, correlation integral is the average no of pair of points where the distance between them is less than  $\varepsilon$ .

As the number of points tends to infinity, and the distance between them tends to zero, the correlation integral for small values of  $\varepsilon$  will take the form;

$$C(\varepsilon) \propto \varepsilon^D \quad (2.11)$$

where  $D$  is known as the *correlation dimension*.

If the number of points is sufficiently large and evenly distributed, gradient of the log-log plot of the correlation integral versus  $\varepsilon$  will yield an estimate of  $D$ .

### 3. RESULTS AND DISCUSSION

#### 3.1 Dependency with $\eta$

The exponent  $\eta$  in DB model parameterizes the relationship between the local electric field and the probability of growth of the discharge pattern. The overall appearance of the pattern and the fractal dimension is strongly related to the exponent  $\eta$  [7]. The following study was carried out in order evaluate the effect of  $\eta$  on the shape and dimension of 2D and 3D discharge patterns. For simplicity, default potential values  $U_{\text{cathode}}=0$  and  $U_{\text{anode}}=1$  were chosen for the cloud base and the ground plane respectively.

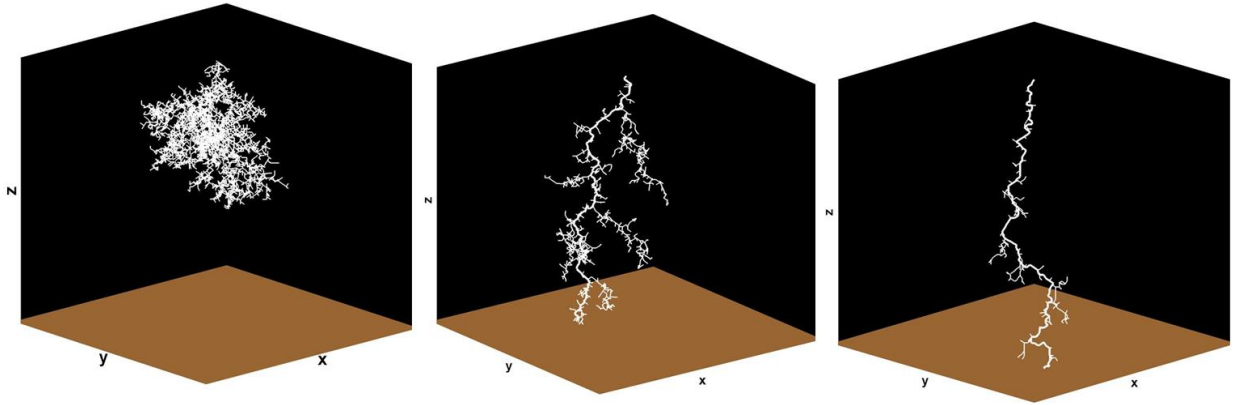


**Figure 3:** Simulated 3D lightning discharge patterns when (a)  $\eta=1$ , (b)  $\eta=3$  and (c)  $\eta=6$

Figure 3 shows lightning discharge patterns for three different  $\eta$  values. It can be seen that as  $\eta$  is increased, discharge patterns become sparser with reduced side branching while for lower values of  $\eta$ , “bush” type densely packed discharge patterns can be observed.

In order to characterize the fractal nature of discharges, fractal dimension of discharge patterns corresponding to different values of  $\eta$  were estimated. To reduce statistical fluctuations, for each value of  $\eta$ , 10 separate simulations were taken and the average fractal dimension  $D$  was calculated. The average fractal dimension values for 2D and 3D configurations are shown on Figure 4. The error bars on the figure represent the standard deviation of the measurements.

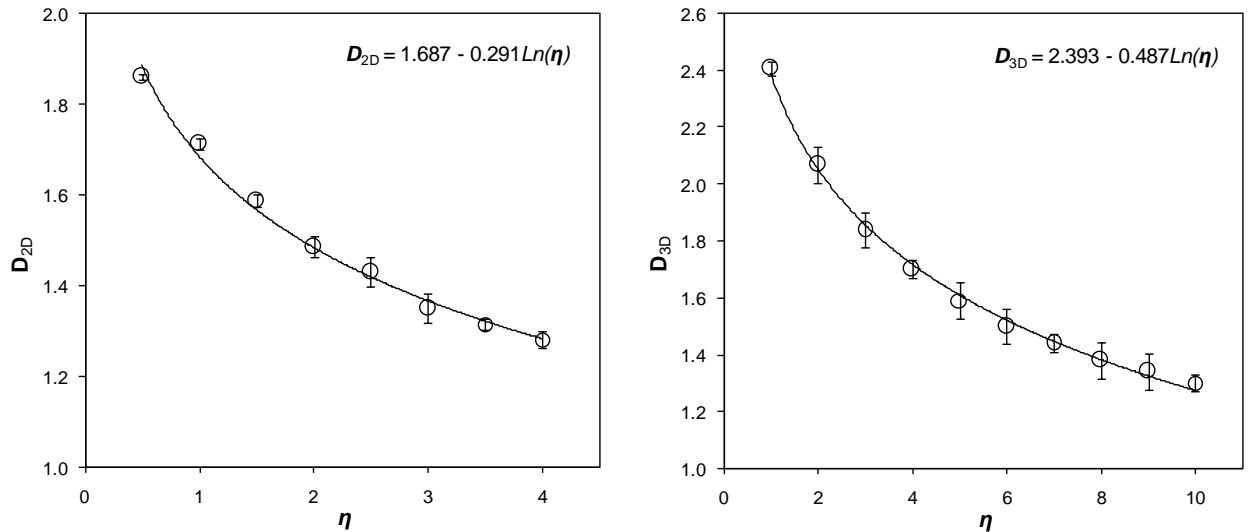


**Figure 4:** Variation of fractal dimension with  $\eta$  for simulated discharges (a) 2D (b) 3D

The relationship between fractal dimension  $D$  and  $\eta$  can be expressed by following expressions.

**2D case:**  $D_{2D} = 1.687 - 0.291 \times \ln(\eta)$  (3.1)

**3D case:**  $D_{3D} = 2.393 - 0.487 \times \ln(\eta)$  (3.2)

Tsonis<sup>4</sup> reported the average 2D fractal dimension estimated from actual lightning photographs to be  $D = 1.34$ . Value of  $\eta$  that produces simulated 2D lightning discharges with the same  $D$  was found to be  $\eta \approx 3.3$ .

In analyzing actual lightning discharges which are in 3D domain, observations are done through 2D lightning photographs. Therefore, to compare simulated 3D lightning discharges with actual discharges, vertical projections of 3D lightning patterns were taken on to either XZ or XY plane and fractal dimension of the projected patterns were estimated.

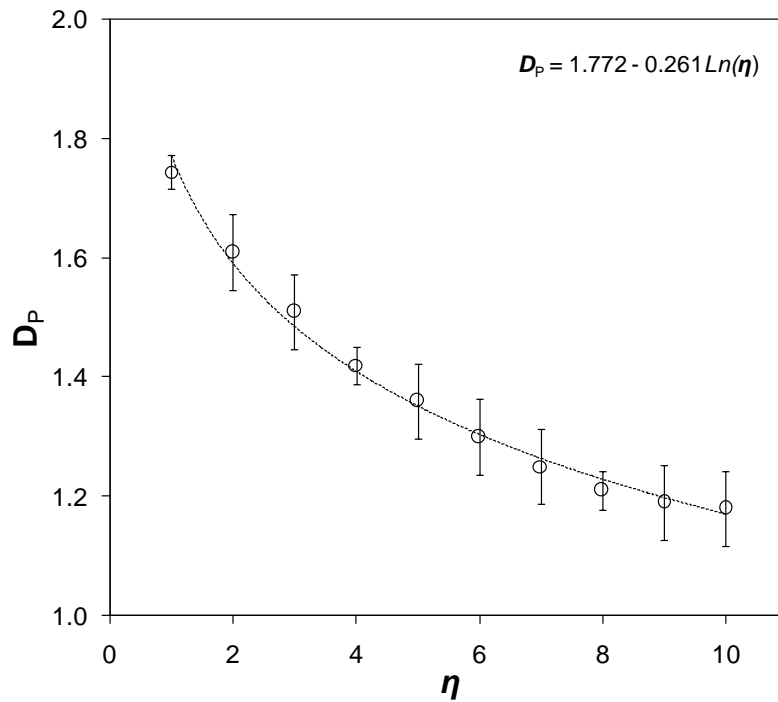


**Figure 5:** Variation of fractal dimension with  $\eta$  for simulated discharges (projected).

The variation of the average fractal dimension of the projected patterns  $D_p$  obtained for various values of  $\eta$  are shown in Figure 5. Similar to the average fractal dimension, exponential decrease in the fractal dimension can be seen with the projected pattern generated with different  $\eta$  values. The relationship between  $D_p$  and  $\eta$  can be given by;

**3D projected case:**  $D_p = 1.772 - 0.261 \times \ln(\eta)$  (3.3)

The average fractal dimension observed for real lightning discharges can be obtained through simulation when  $\eta = 5.2$ . This value is close to the value reported by a similar study carried out by Sanudo et al.<sup>15</sup>.

### 3.2 Influence of ground objects on lightning flashes

One of the most important features of DB model is that it allows the use of attractors and repulses to direct the growth of the discharge pattern. The growth can be attracted to a user specified region by setting the boundary condition  $\phi = U_{\text{anode}}$  for the lattice points occupied by that region, while the growth can be repulsed from the region by setting  $\phi = U_{\text{cathode}}$ . For the two lattice configurations used in this study, initial boundary conditions imposed by the ground plane and cloud base themselves act as an attractor and a repulsor respectively. Furthermore, by introducing additional attractors and repulsors, the direction of propagation of the discharge can be controlled accordingly. In this study, additional attractors were introduced into the 3D lightning configuration to simulate the effect of objects on the ground plane during lightning flashes. In order to impose realistic conditions for lightning discharges,  $\eta = 5.2$  was used. For simplicity, default values  $U_{\text{cathode}} = 0$  and  $U_{\text{anode}} = 1$  were used to represent the potential of cloud base and ground respectively.

Figure 6 shows final visual output of two simulations conducted to demonstrate the behaviour of simulated lightning discharges near ground objects. Additional boundary conditions imposed by these structures were incorporated by setting the potential of the lattice points occupied by the grounded structures to  $\phi = 1$ . In both simulations, lightning discharge was attracted towards the grounded structure, instead of the ground plane. The obvious reason behind such behavior is that the local electric field near the pointed surfaces of the structures is relatively higher than that of the ground plane. Since the growth probability of the discharge is dependent on local electric field, propagation of the pattern gets oriented towards the areas of high local electric field.

Due to its stochastic nature, the exact strike path of real lightning flashes is unpredictable<sup>13</sup>. Although taller pointed structures on the ground have a higher probability to be struck by lightning, predicting whether lightning flashes initiated from a nearby cloud base will hit the structure is not possible. In order to justify that the same stochastic property is conserved in DB model as well, a simple analysis was conducted using the grounded vertical rod shown in Figure 6a.

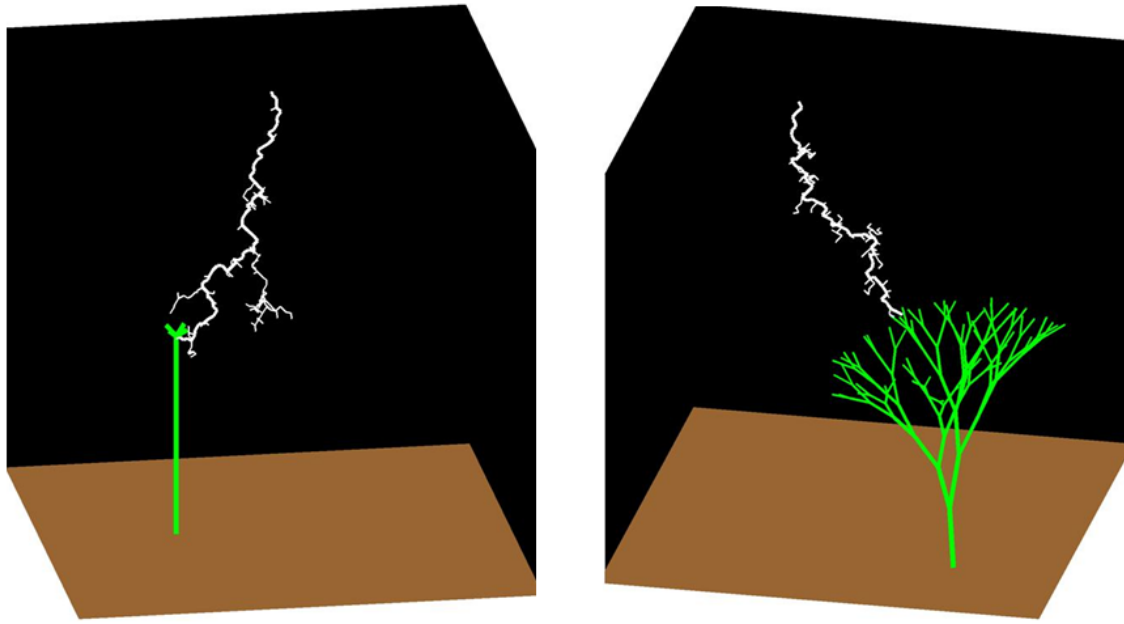


**Figure 6:** Simulated lightning discharges striking objects on the ground. (a) A simple vertical rod (b) A complex tree-like structure.

By varying the height ( $h$ ) of the rod and the horizontal distance ( $d$ ) from the discharge initiation point, a set of simulations were carried out to determine the frequency of lightning strikes. Twenty simulations were carried out for each combination of  $h$  and  $d$ , and the number of times the rod was struck by lightning was counted for each case. The results are given in Table 1. All lengths and heights are given in terms of the nearest neighbor distance of the lattice.

**Table 1:** Frequency of lightning strikes on the rod for various values of  $h$  and  $d$

$h$	$d$	No of strikes (out of 20)	Probability of lightning strike
45	20	15	0.75
40	20	12	0.60
30	20	10	0.50
30	30	6	0.30
30	35	4	0.20

The data given in Table 1 show that lightning flash hitting the rod is not a deterministic event. Although the data sample is limited, for every combination of  $h$  and  $d$  considered, probability of a lightning strike is less than 1; that is there's always a non zero probability for the simulated lightning flash to miss the rod and hit the ground nearby. However, probability of striking the rod seems to be dependent on the height ( $h$ ) of the

rod and the horizontal distance ( $d$ ) from the discharge initiation point. Probability of a strike appears to increase with height of the rod. This observation agrees with the situation regarding real lightning strikes; that the probability of taller objects getting hit by lightning is higher than that of shorter objects. Also it can be noticed that the probability of a strike decreases as the horizontal distance to the discharge initiation point ( $d$ ) is increased; which is also a situation one can expect in real lightning.

The results of simulations suggest that DB model posses the same stochastic properties observed in real lightning. This behaviour is expected due to the probabilistic manner in which new links are added to the discharge structure. An important thing to consider here is that the ratio between the height of a ground object, and the distance between ground and cloud base in the simulations may not be comparable with the real situation. Therefore one should not attempt to directly compare the results given in Table 1 with situations regarding real lightning strikes.

### 3.3 Upward connecting positive leader development

Upward connecting positive leader development which occurs during real CG lightning flashes can be effectively simulated with the novel extension introduced into DB model. As done in the previous section, in order to impose realistic conditions for lightning discharges,  $\eta = 5.2$  was used and the default initial boundary conditions  $U_{\text{cathode}} = 0$  and  $U_{\text{anode}} = 1$  were used for simplicity.

Although the breakdown physics are different for negative stepped leaders and upward connecting positive leaders<sup>13</sup>, for simplicity, both types of discharges were treated in the same way in this work. That is, the value of  $\eta$  used to control stepped leader growth ( $\eta = 5.2$ ) was used to control upward connecting leader growth as well. However it should be noted that one can change the growth and appearance of upward connecting positive leaders by simply giving a different value of  $\eta$ .

Figure 7 shows a snapshot taken from a simulation conducted to demonstrate upward connecting positive leader development from the ground plane. The negative stepped leader is indicated in blue while the upward connecting positive leaders are in red. At the time when the snapshot was taken, two upward connecting leaders appear to have developed from the ground plane. The threshold for upward connecting leader initiation was set to  $E_{\text{break}} = 0.02$ . The first upward connecting leader initiated from the ground, when the tip of the stepped leader approached at a height of 23 units from the ground (cloud base is at 100 units). At a height of 17 units from the ground, the longest upward connecting positive leader intercept with the negative stepped leader, forming the complete lightning path.

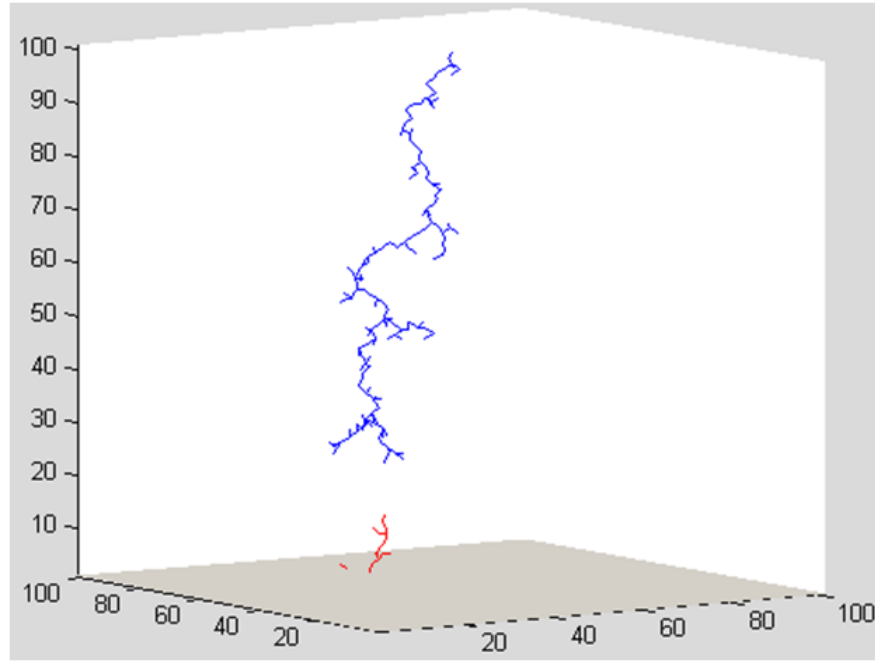


**Figure 7:** Upward connecting positive leader developing from earth surface.

It was assumed that the threshold  $E_{break}$  controls the height to the stepped leader tip from the ground, when the upward connecting leader initiation occurs. In order to test this hypothesis,  $E_{break}$  was varied from 0.02 to 0.07, and for each case, height of the leader tip above the ground ( $H$ ) at the time when the first upward connecting leader initiated was determined. To reduce statistical fluctuations, 10 simulations were executed for each value of  $E_{break}$  and average height  $H$  was calculated. The variation of  $H$  versus  $E_{break}$  is shown in Figure 8. The errors indicated in the figure are the errors in the mean calculated as  $\sigma = s / \sqrt{n}$  where  $s$  is the standard deviation and  $n$  is the number of measurements. Since the growth of the discharges occurs in discrete steps,  $H$  takes only integer values. Therefore average height  $H$  was truncated to the nearest integer.

Figure 8 clearly shows that the average height  $H$  exponentially decreases with  $E_{break}$ . This behaviour is quit logical since the role of  $E_{break}$  is to suppress the effect of local electric field when selecting initial discharge links for new upward connecting leaders. As the stepped leader approaches at a certain height from the ground, local electric field associated with one or more possible breakdown links (that are relevant to upward connecting leader initiation) will exceed  $E_{break}$ , initiating upward connecting leaders. But if  $E_{break}$  is increased, a much higher value of local electric field may be needed to surpass it, and the stepped leader may need to descend further down to produce that same effect.



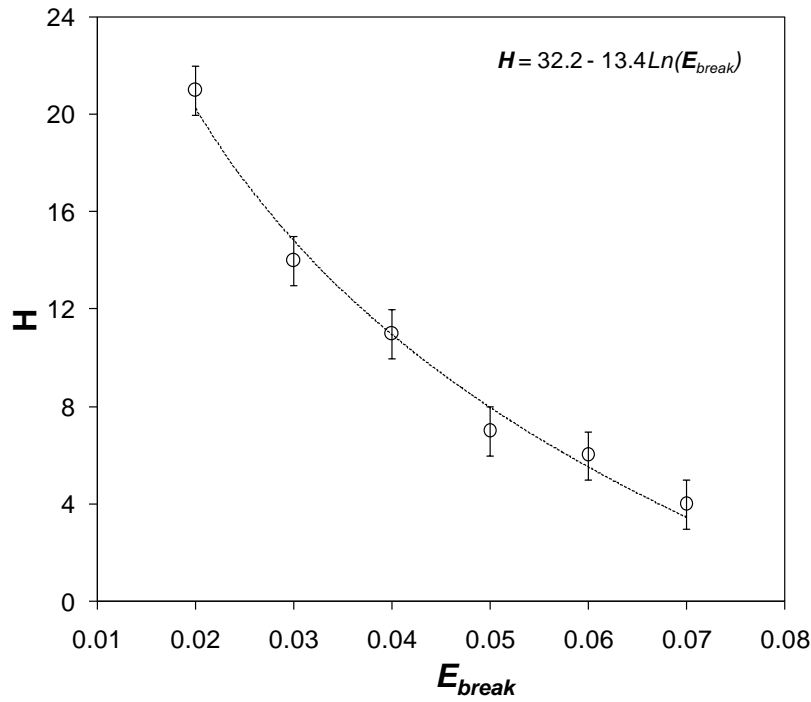


**Figure 8:** Variation of  $H$  as a function of  $E_{break}$

#### 4. CONCLUSIONS

In this work, stochastic dielectric breakdown model was applied to both 2D and 3D domains to simulate lightning discharges. Important results obtained in this work are summarized as follows:

- Appearance and fractal dimension of discharge patterns are strongly dependent on the model parameter  $\eta$ . For large values of  $\eta$ , “branched” type discharges are formed while lower values of  $\eta$  produces “bush” type (densely packed) discharges.
- As  $\eta$  is increased, average fractal dimension of the patterns decrease exponentially. 3D discharge patterns similar to the actual lightning are obtained when  $\eta \approx 5.2$ .
- By introducing additional boundary conditions into DB model, influence of ground objects on lightning flashes can be simulated. Tall, pointed structures on the ground have a higher probability of attracting simulated lightning discharges. Probability of strikes increases with the height of the ground object while it decreases as the horizontal distance to the discharge initiation point is increased.
- A new extension introduced into the DB Model can simulate the development and attachment of upward connecting positive leaders to the downward moving negative stepped leader during the progression of CG lightning flashes. Height of the stepped leader tip above the ground (at the time when the upward connecting leader initiation occurs) is dependent on the initial breakdown voltage threshold. Average height to the point of inception decreases exponentially as breakdown threshold increases.

## Acknowledgements:

Financial assistance by National Science Foundation (research grant number RG/04/E/06) is acknowledged.

## REFERENCES

1. L. Niemeyer, L. Pietronero, H.J. Wiesmann, *Fractal dimension of dielectric breakdown*, Physical Review Letters 52, (1984) 1033-1036
2. D. Amarasinghe, U. Sonnadara, M. Berg, V Cooray, *Channel tortuosity of long laboratory sparks*, J. Electrostatics 65, (2007) 521-526
3. B. Mandelbrot, *The Fractal Geometry of Nature*. W. H. Freeman and Co. New York (1982).
4. A.A. Tsonis, *A fractal study of dielectric breakdown in the atmosphere*. In: *Scaling, Fractals and Non Linear Variability in Geophysics* (eds. D. Schertzer & S. Lovejoy), Kluwer Academic Publishers, Netherlands, pp. 167-174..
5. J. Sanudo, J.B. Gomez, F. Castano, A.F. Pacheco, *Fractal dimension of lightning discharge*, Nonlinear Processes in Geophysics 2, (1995) 101-106
6. D. I. Amarasinghe, D.U.J. Sonnadara, *Fractal characteristics of simulated electrical discharges*, J. of National Science Foundation, 36, (2008) 137-143
7. K. Kudo, *Fractal analysis of electrical trees*, IEEE Transactions on Dielectrics and Electrical Insulations 5, (1998) 713-726.
8. E.R. Mansell, D.R. MacGorman, L.C. Ziegler, J.M. Straka, *Simulated three-dimensional branched lightning in a numerical thunderstorm model*. J. Geophysical Research 107(D9), (2002) 4075
9. T. Kim, M.C. Lin, *Physically based animation and rendering of lightning*, Proceedings of the 12<sup>th</sup> Pacific Conference on Computer Graphics and Applications, (2004) 267-275.
10. T. Kim, J. Sewal, A. Sud, M.C. Lin, *Fast Simulation of laplacian growth*, IEEE Computer Graphics and Applications 27, (2007) 68-76.
11. J.W. Duncan, *The accuracy of finite-difference solutions of laplace's equation*, IEEE Transactions on Microwave Theory and Techniques 15, (1967) 575-582.
12. A.L. Barclay, P.J. Sweeney, L.A. Dissado, G.C. Stevens, *Stochastic modelling of electrical treeing: fractal and statistical characteristics*, Journal of Physics D: Applied Physics 23, (1990) 1536-1545
13. J.P. Liyanage, *Correlation between optical and current signatures of electrical discharges with special attention to remote sensing of lightning flashes*. Ph.D. Thesis, University of Colombo, Sri Lanka (2006).